



Optimal Design of VLH Axial Hydro-Turbine using Regression Analysis and Multi-Objective Function (GA) Optimization Methods

W. Nuantong¹ and S. Taechajedcadarungsri^{2†}

¹ Department of Mechanical Engineering, Faculty of Engineering, Khon Kaen University, 40002, Thailand

² Department of Mechanical Engineering, Faculty of Engineering, Ubon Ratchathani University, 34190, Thailand

†Corresponding Author Email: sirivit.t@ubu.ac.th

(Received August 12, 2015; accepted December 22, 2015)

ABSTRACT

This research study was aimed to develop a new concept design of a very low head (VLH) turbine using advanced optimization methodologies. A potentially local site was chosen for the turbine and based on its local conditions, such as the water head level of <2 meters and the flow rate of <5 m³/s. The study focused on the optimization of the turbine blade and guide vane profiles, because of their major impacts on the efficiency of the VLH axial flow turbine. The fluid flow simulation was firstly conducted for the axial turbine, followed by applying the regression analysis concept to develop a turbine mathematical model where the leading- and trailing-edge angles of the guide vanes and the turbine blades were related to the efficiency, total head and flow rate. The genetic algorithms (GA) with multi-objective function was also used to locate the optimal blade angles. Thereafter, the refined design was re-simulated. Following this procedure the turbine efficiency was improved from 82.59% to 83.96% at a flow rate of 4.2 m³/s and total head of 2 meters.

Keywords: Blade angle; Regression analysis; Fluid flow simulation; Optimization; Genetic algorithm; Very low head turbine.

1. INTRODUCTION

A design concept of a turbine is mostly dependent on conditions of installation and performance. Computational fluid dynamics (CFD) methods are frequently used to analyze the flow field in turbomachinery (Benajes *et al.* 2014, Chen *et al.* 2005, Lazari and Cattanei 2014, Mokaramian *et al.* 2015), such as axial flow turbine. When coupled with optimization concepts, the design of a hydro turbine leads to superior results, compared to traditional methods. The multi-objective technique based on genetic algorithm is a potential tool to support a determination of the optimal shape of turbine blades and vanes. On parameter analysis, Lipej (Lipej 2004) combined either linear or higher-order functions with common variables, such as (a) the meridional velocity coefficient (two variables), (b) the outlet vortex coefficient (two variables), (c) the chord-pitch ratio (two variables), (d) the relative profile maximum thickness (two variables), and (e) the camber position (two variables) from hub to the maximum radius of the runner. By applying multi-objective functions on the blade profile, guide vane and the stay vane, the turbine efficiency was increased by 3% and the output power was also

enhanced by 13%. In this case, the optimal design of the turbine also avoided the cavitation effect (Wu *et al.* 2006). Albuquerque *et al.* (2007) applied optimization techniques, standard sequential quadratic programming, and the controlled random search algorithm for the design parameters of runner blade stagger, camber and chord-pitch ratio at the hub, mean, and tip stations. These works demonstrated an improvement of overall performance. Specific design parameters, namely (1) total pressure at the inlet and outlet, (2) outlet angle, and (3) surface spiral casing, when applying evolutionary algorithms to the design of stay vanes and guide vanes, brought about turbine performance improvement (Alnaga and Kueny 2008). Simulation of CFD model at specific speeds of 81 and 48 using the new design parameters showed that the turbine efficiency improved by 1.5% and the surface spiral casing dropped by 3-5% with the reduction of the power loss by 1-2%, compared to the initial design. The automatic process of the Nelder-Mead Simplex method was used to determine the blade shape with the minimum objective function comprising efficiency, head and cavitation (Skotak *et al.* 2009). The change of the reference axes and the angle coordinates with B-spline curve of the modified

blade caused a proper distribution of pressure and flow velocity on the blade surface and increased the turbine efficiency to 93.3% (Yang *et al.* 2011). The efficiency of the turbine from the CFD simulations, at the initial conditions of 1.8 bar of total pressure, with a torque of 402 N-m and 19 meters of head, was 67.4% before optimization. By changing blade profile parameters (thickness, hub length, chord length, chord angle and hub angle), an optimization technique was applied using an orthogonal array and analysis of variance, with a polynomial equation for a surrogate model. The blade efficiency improved to 71.2% with a torque of 313.7 N-m and a head of 15.5 meters (Jung *et al.* 2012). The efficiency of the turbine runner was superior by using CFD simulation, and verified by making a comparison between curved edge and straight edge blades. Despite of a slight change in turbine efficiency, the curved edge blade increased the flow rate more than a straight edge. Ge *et al.* (2013) reported the twist angle of the blade not only affected the flow rate and torque, but also the efficiency and power output. The results led us to focus on optimal blade angle for further investigation.

The purpose of this work was therefore to use the CFD for simulation of the axial turbine in order to solve the flow problem. Optimization techniques were subsequently applied to improve the turbine efficiency and determine the optimal blade profile. In addition, regression analysis was also employed to develop a mathematical model of relationships between the blade angles (eight variables) of both leading and trailing edges of guide vanes and turbine blades, with a particular emphasis on efficiency, total head and flow rate. The mathematical model was applied to create a multi objective minimum function. GA technique was utilized to find the guide vane angles and the turbine blade angles for an optimal design of the axial turbine at the low head of not more than 2 meters and the flow rates below 5 m³/s.

2. CFD SIMULATION AND VALIDATION

A rotating reference frame was used to simulate the flow in the turbine. Since the realizable $k-\epsilon$ model with enhanced near-wall treatment is an efficient turbulence model that has shown acceptable results for simulating the flow field in hydro-turbines (Kaniecki *et al.* 2011, M. Ramos *et al.* 2013, Sutikno and Adam 2011), it was then applied to investigate the flow effect on the blade performance in our work. Numerical analysis was carried out using the ANSYS Fluent software for hydro-turbine simulations.

To verify the CFD results, the turbine was initially set to have a diameter of 100 mm and five blades. M. Ramos *et al.* (2013) validated their experimental results by using the turbine blade profiles, which was described by the blade angles. In our approach the results of CFD simulation agreed well with their work, as shown in Fig. 1.

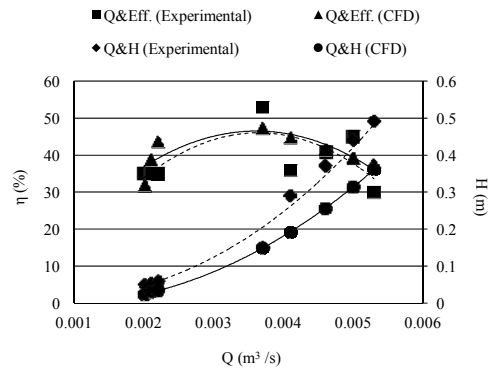


Fig. 1. Characteristic curves of CFD and experiment.

Figure 1 shows comparison of relationships between head versus flow rate, and turbine performance versus flow rate for the CFD simulation and experimental results. The efficiencies from the experiment were more scattering than those from CFD at the same flow rate. However, both efficiency data sets were similarly distributed, as shown by the performance curves. In practice the experimental efficiency is lower than that of CFD simulation for the same flow rate, as a result of the energy loss of the turbine system. At a flow rate of 0.0037 m³/s, the maximum efficiency obtained by CFD computation was 47.22 %, lower than the experimental value by 5.78 %. Fluctuations of the actual reading also caused discrepancies between the two efficiency data sets, while the system curves from both methods gave similar trends.

When using the same turbine profiles and boundary conditions, the data set of simulation and experimental results (from M. Ramos *et al.* (2013)) were consistent, the CFD simulation results were therefore considered valid for further investigations in optimization of blade profile.

3. CFD OF EXPERIMENTAL TURBINE

3.1 Geometry Design

In this element of the work, the axial turbine consisted of 12 guide vanes and 5 runner blades. Initial conditions were defined for the water head level of <2 meters with the flow rate of <5 m³/s, and they were applied to the Bernoulli equation as shown in Eq. (1),

$$V = \sqrt{2gH} \tag{1}$$

The mean axial velocity (v) is written as a function of the flow rate (Q) in the sectional area of rotor blade (A), as shown in Eq. (2),

$$Q = V \times A \tag{2}$$

The sectional area of rotor blade (A) is expanded as,

$$A = \left(\frac{\pi D^2}{4}\right) \times \left(1 - \left(\frac{d_h}{D}\right)^2\right) \tag{3}$$

Therefore, from Eqs. (1), (2) and (3), we can define Q as given in Eq. (4),

$$Q = \sqrt{2gH} \times (\pi D^2/4) \times (1 - (d_h/D))^2 \quad (4)$$

The diameter ratio (hub to tip ratio, d_h/D) of the axial turbine is typically 0.4 to 0.55 (Alexander *et al.* 2009, Ferro *et al.* 2011, F. Round 2004, Singh and Nestmann 2011). In our case the diameter ratio was therefore selected at 0.48, which was the median. Eq. (4) was used for a tip diameter of 1.15 meters and a hub diameter of 0.55 meters. The ANSYS Workbench software was employed to create the axial turbine model, as shown in Fig. 2.

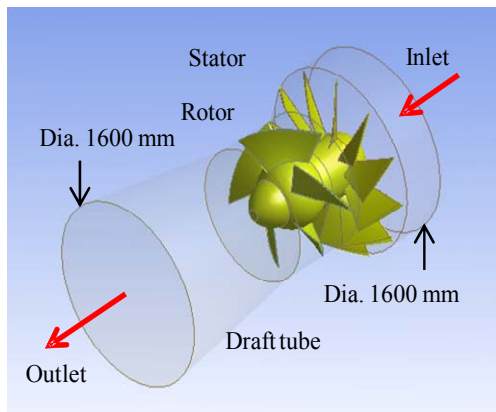


Fig. 2. Characteristic of the axial turbine model.

The guide vane angle was defined by variables β_1 and β_2 at the hub position, with the tip position defining the variables β_3 and β_4 . The turbine blade angle was defined by variables β_5 and β_6 at the hub position, and the tip position was defined by variables β_7 and β_8 , as shown in Fig. 3.

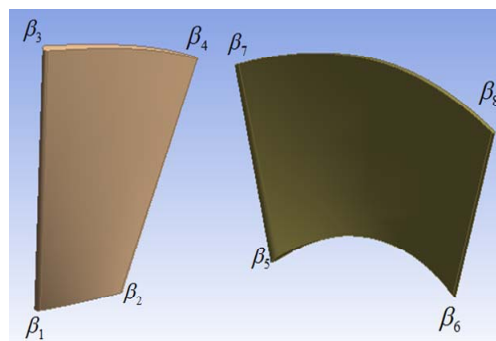


Fig. 3. Definition of the guide vane angles and the blade angles.

By using the Latin hypercube sampling (LHS) method, the angles of guide vanes and turbine blades were randomized, generating thirty models. In this method, the domain of each random variable was decomposed into intervals and the same

probability was assigned to all intervals. The number of intervals depended on the number of samples generated for each variable. One value from each interval was randomly selected with respect to the probability density of interval. To form the hypercube combination, the interval of random variable is performed. When sampling a function of N variables, the range of each variable is divided into M equally probable intervals. M sample points are then placed to satisfy the Latin hypercube requirements; this restricted the number of divisions M, to be equal for each variable. The maximum number of combinations for a Latin hypercube of M divisions and N variables can be computed using the relationship given in Eq. (5),

$$\left(\prod_{n=0}^{M-1} M - n \right)^{N-1} = (M!)^{N-1} \quad (5)$$

The governing equation is given in Eq. (6),

$$pf = \frac{1}{N} \sum_{k=1}^N I_g(x_k) \quad (6)$$

where, pf is the expected probability of failure, and $I_g(x_k)$ is an indicator of sample x of k^{th} number. The value of the indicator will be 1 if the system is not satisfied, otherwise 0 (Chakraborty 2015).

Table 1 shows the randomized angles of guide vanes and turbine blades obtained by LHS method. For the guide vane, the thickness of the leading and trailing edge was 10 and 5 mm, respectively, while those for the turbine blade were 20 to 5 mm at the hub, and 15 to 5 mm at the tip. The initial thickness of the guide vane and the turbine blade were defined by limits on material and manufacturing constraint.

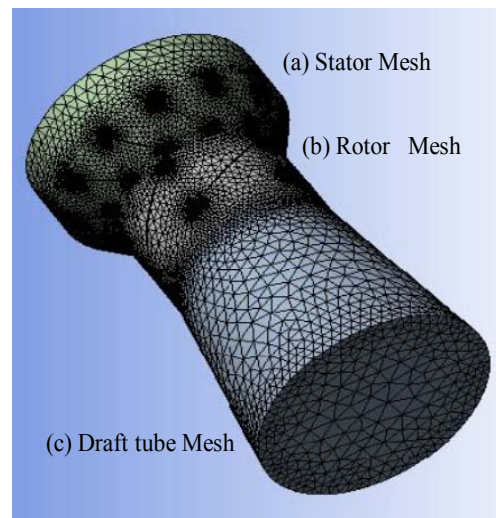


Fig. 4. Mesh construction.

3.2 Meshing of the Axial Turbine

In Fig. 4 the mesh domain constructed from 5,983,523 elements consists of (a) stator, (b) rotor

Table 1 Angles (β) in degree from the sampling technique and simulation results for thirty turbine models

Model	Angles (degree)								Simulation results				
	β_1	β_2	β_3	β_4	β_5	β_6	β_7	β_8	Q (m ³ /s)	H_{total} (m)	τ (N-m)	η (%)	Output (kW)
1	11.2	22.7	34.8	49.2	29.2	42.3	46.7	55.5	4.66	1.78	2,598.05	66.93	54.39
2	17.5	21.1	36.9	48.1	29.6	39.3	48.4	61.6	4.31	1.71	2,667.02	77.45	55.83
3	12.1	29.7	38.1	44.5	33.6	38.7	45.8	57.0	4.58	1.77	2,247.11	59.14	47.04
4	16.2	20.1	32.5	44.0	26.6	42.9	47.3	59.7	4.65	1.81	3,136.53	79.48	65.66
5	18.0	20.8	31.4	40.4	27.8	44.4	50.5	63.6	4.39	1.95	3,308.74	82.59	69.26
6	19.9	24.4	32.8	46.7	27.5	36.0	50.8	58.5	4.58	1.77	2,889.60	76.19	60.49
7	15.9	25.1	33.1	42.8	25.9	43.6	51.1	56.5	4.72	1.83	3,133.82	77.54	65.60
8	19.4	26.7	34.5	44.9	34.7	44.8	45.3	59.3	4.48	1.86	2,784.23	71.35	58.28
9	18.4	28.5	35.4	42.3	34.4	39.6	48.1	59.5	4.58	1.84	2,975.24	75.40	62.28
10	19.0	25.6	32.2	48.4	26.1	43.8	47.6	63.7	4.16	1.81	2,878.03	81.49	60.25
11	17.0	26.4	36.4	47.4	32.5	36.3	53.5	62.2	4.16	1.74	2,687.91	79.31	56.27
12	13.2	21.9	33.8	41.8	31.3	41.1	53.8	57.9	4.66	1.83	3,188.09	79.74	66.74
13	17.9	20.4	38.4	49.0	30.6	43.0	52.0	64.1	4.00	1.86	2,811.32	80.94	58.85
14	14.2	29.1	31.7	49.8	34.1	35.5	54.9	60.6	4.25	1.86	2,914.34	79.00	61.01
15	10.2	24.0	35.3	46.8	30.1	40.3	49.2	57.3	4.63	1.80	2,918.73	74.78	61.10
16	12.0	28.1	30.7	43.7	28.3	38.1	50.3	56.0	4.82	1.79	2,929.53	72.63	61.32
17	14.7	27.0	38.9	43.5	31.6	40.8	50.0	60.7	4.39	1.81	2,921.77	78.78	61.16
18	15.3	23.7	31.2	40.1	28.9	41.6	47.8	62.7	4.55	1.88	3,266.13	81.64	68.37
19	16.4	23.0	39.7	45.7	27.1	36.7	45.4	58.7	4.61	1.72	2,667.05	71.73	55.83
20	10.5	23.4	37.1	46.2	33.7	40.0	53.2	62.5	4.20	1.82	2,896.53	80.97	60.63
21	12.7	22.4	33.4	49.4	33.0	44.3	54.3	61.0	4.20	1.89	3,044.84	81.87	63.74
22	13.9	24.7	39.0	42.5	26.9	36.5	51.6	60.1	4.47	1.69	2,719.31	76.87	56.92
23	11.3	28.9	34.1	47.0	25.7	41.7	46.5	63.3	4.26	1.81	2,927.69	81.19	61.29
24	15.6	26.3	39.6	40.9	31.7	37.2	48.9	64.9	4.21	1.77	2,743.95	78.77	57.44
25	11.0	26.0	30.9	41.6	30.9	42.5	54.7	55.1	4.81	1.85	3,260.86	78.22	68.26
26	19.0	29.4	30.2	45.1	29.8	40.7	49.5	58.1	4.57	1.84	2,854.30	72.59	59.75
27	14.7	27.8	37.5	45.5	25.3	35.3	52.2	57.5	4.53	1.80	2,655.82	69.72	55.60
28	16.8	27.5	36.1	43.2	32.1	38.0	52.4	64.7	4.10	1.80	2,809.71	81.17	58.82
29	12.4	21.5	35.8	41.0	28.5	38.6	46.0	61.7	4.62	1.75	2,956.04	78.26	61.88
30	13.4	22.1	37.9	47.8	33.1	37.5	52.7	56.2	4.57	1.75	2,759.99	73.90	57.78

and (c) draft tube, and they were connected by using a mesh interface. The mesh refinement was performed in order to validate the meshing results, and the efficiencies of turbine at different mesh elements were identified (Fig. 5). Within $\pm 0.65\%$ uncertainty, approximated 6 million element model was chosen to improve the computational cost and efficiency.

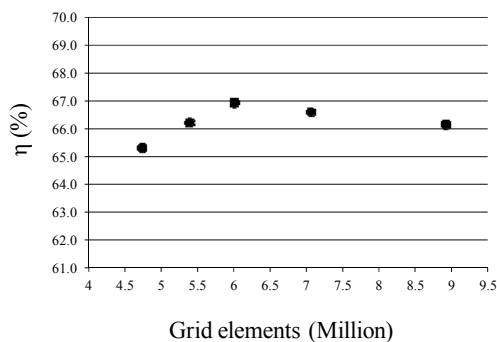


Fig. 5. Simulation results at different mesh refinements.

3.3 CFD Simulation Results

The CFD simulation of the water flow into the axial turbine was performed by using the water density of 998.2 kg/m³. The assumption was set for an incompressible flow, excluding the cavitation. The rotating speed of the runner blade was 200 rpm,

related to the moving reference frame.

From the results of simulation of thirty models in Table 1, the maximum turbine efficiency was 82.59% at the flow rate of 4.39 m³/s and total head of 1.95 meters. The torque on the runner blade was 3,308.74 N-m and the maximum power output was 69.26 kW. The guide vane and the turbine blade defining angles, β_1 to β_8 , were 18°, 20.8°, 31.4°, 40.4°, 27.8°, 44.4°, 50.5° and 63.6° respectively, as shown in Fig. 3 and Table 1. Characteristics of velocity and pressure in the axial turbine in Figs. 6 and 7 agreed well with the theory of fluid machinery. For the turbine blades, the leading edge had higher pressure on the side than that on the trailing edge by a factor of 2.86. For the trailing edge of the suction side, the pressure was low (-18,091.05 Pa).

4. REGRESSION ANALYSIS FOR MATHEMATICAL MODEL

We defined the eight angles of guide vane and turbine blade as independent variables, with the basic parameters, namely efficiency, total head and flow rate, as dependent variables for the regression analysis. A mathematical model was then applied to linear regression, which describes the relationship between independent and dependent variables in the equation.

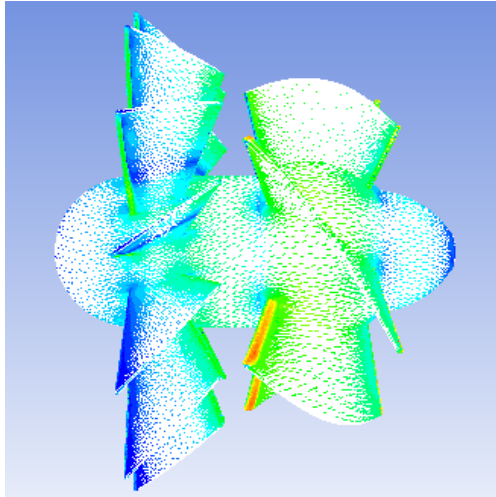


Fig. 6. Velocity in the axial turbine.

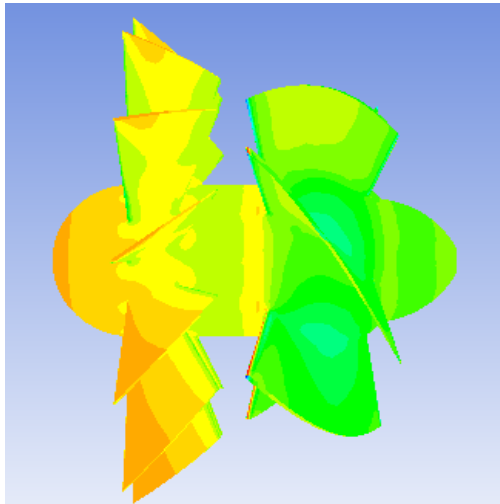


Fig. 7. Static pressure on the axial turbine.

$$Y' = c_0 + \sum_{i=1}^n c_i X_i + e \tag{7}$$

where Y' is dependent variable, $X_i (i = 1, \dots, n)$ are independent variables, $c_i (i = 0, \dots, n)$ are regression coefficients and e is the error associated with the regression.

A prediction of the regression model (Y) is calculated by

$$Y = c_0 + \sum_{i=1}^n c_i X_i \tag{8}$$

In Eqs. (7) and (8) (Pires *et al.* 2008, Sun and Bertrand-Krajewski 2012), the error (e) is the difference between actual and predicted values as shown in Eq. (9),

$$e = Y' - Y \tag{9}$$

Tables 1 also shows the results of regression analysis with the level of significance at 0.05. Both

adjusted R^2 and F value were compared for four models of the relationship equations, as shown in Table 2 to 4.

Among all proposed models, the multiple linear regression had higher adjusted R^2 and F values than the others, obtaining the optimal equation for the relationships between the angle of guide vane and turbine blade. The relationship of performance and flow rate was also linear. However, from Table 3, the optimal relationship of total head and the angles is non-linear with a double log model.

The equations relating the performance, total head and flow rate to the regression coefficients are given in Eqs. (10), (11) and (12) respectively,

$$\eta = -3.704 - 0.089\beta_1 - 0.382\beta_2 - 0.438\beta_3 - 0.195\beta_4 - 0.245\beta_5 + 0.199\beta_6 + 0.795\beta_7 + 1.249\beta_8 \tag{10}$$

$$H_{total} = \frac{(\beta_1^{0.011} \times \beta_2^{0.036} \times \beta_5^{0.055} \times \beta_6^{0.25} \times \beta_7^{0.14} \times \beta_8^{0.105})}{10^{0.412} \times \beta_3^{0.136} \times \beta_4^{0.055}} \tag{11}$$

$$Q = 12.058 - 0.004\beta_1 - 0.013\beta_2 - 0.018\beta_3 - 0.029\beta_4 - 0.003\beta_5 - 0.013\beta_6 - 0.019\beta_7 - 0.061\beta_8 \tag{12}$$

From Eqs. (10), (11) and (12), the adjusted R^2 for functions of performance, total head and flow rate were 0.759, 0.646 and 0.986 respectively.

5. TURBINE OPTIMIZATION

To optimize the blade shape the minimum objective function of parameters of efficiency, head and cavitation were employed (Skotak *et al.* 2009). In this study, the objective function utilized the efficiency, total head and flow rate parameters in the functional equation, as shown in Eqs. (10), (11) and (12), and the optimization by using genetic algorithms (GA) is shown in Eq. (13).

$$f \min = W_1 \left[1 - \left(\frac{\eta(\beta_i)}{100} \right) \right] + W_2 \left[\frac{|H_c - H_{total}(\beta_i)|}{H_{total}(\beta_i)} \right] + W_3 \left[\frac{|Q_c - Q(\beta_i)|}{Q(\beta_i)} \right] \tag{13}$$

Find: $\beta_1, \beta_2, \beta_3, \beta_4, \beta_5, \beta_6, \beta_7, \beta_8$, to minimize $f \min = f(\eta(\beta_i), H_{total}(\beta_i), Q(\beta_i))$,

subject to constraint,

$$\eta(\beta_i) \leq 100\%, H_{total}(\beta_i) \leq 2m, Q(\beta_i) \leq 5m^3/s, i = 1, 2, \dots, 8$$

for initial conditions of the design, $H_c = 2m$,

Table 2 Relationship equations between the efficiency and the angle

Method model*	Equation	Adjusted R ²	F
1. Multiple linear regression	$\eta_i = c + \lambda_1\beta_{1i} + \lambda_2\beta_{2i} + \dots + \lambda_8\beta_{8i}$	0.759	12.408
2. Double log	$\log \eta_i = \log c + \lambda_1 \log \beta_{1i} + \dots + \lambda_8 \log \beta_{8i}$	0.686	8.933
3. Semi- log	$\log \eta_i = c + \lambda_1\beta_{1i} + \lambda_2\beta_{2i} + \dots + \lambda_8\beta_{8i}$	0.721	10.373
4. Reciprocal	$\eta_i = \frac{1}{c + \lambda_1\beta_{1i} + \lambda_2\beta_{2i} + \dots + \lambda_8\beta_{8i}}$	0.683	8.821

* Significance = 0.000 for every model.

Table 3 Relationship equations between the total head and the angle

Method model*	Equation	Adjusted R ²	F
1. Multiple linear regression	$H_{total\ i} = c + \lambda_1\beta_{1i} + \lambda_2\beta_{2i} + \dots + \lambda_8\beta_{8i}$	0.609	6.646
2. Double log	$\log H_{total\ i} = \log c + \lambda_1 \log \beta_{1i} + \dots + \lambda_8 \log \beta_{8i}$	0.646	7.606
3. Semi-log	$\log H_{total\ i} = c + \lambda_1\beta_{1i} + \lambda_2\beta_{2i} + \dots + \lambda_8\beta_{8i}$	0.623	6.999
4. Reciprocal	$H_{total\ i} = \frac{1}{c + \lambda_1\beta_{1i} + \lambda_2\beta_{2i} + \dots + \lambda_8\beta_{8i}}$	0.626	7.078

* Significance = 0.000 for every model.

Table 4 Relationship equations between the flow rate and the angle

Method model*	Equation	Adjusted R ²	F
1. Multiple linear regression	$Q_i = c + \lambda_1\beta_{1i} + \lambda_2\beta_{2i} + \dots + \lambda_8\beta_{8i}$	0.986	258.684
2. Double log	$\log Q_i = \log c + \lambda_1 \log \beta_{1i} + \dots + \lambda_8 \log \beta_{8i}$	0.969	113.893
3. Semi-log	$\log Q_i = c + \lambda_1\beta_{1i} + \lambda_2\beta_{2i} + \dots + \lambda_8\beta_{8i}$	0.985	242.611
4. Reciprocal	$Q_i = \frac{1}{c + \lambda_1\beta_{1i} + \lambda_2\beta_{2i} + \dots + \lambda_8\beta_{8i}}$	0.982	202.884

* Significance = 0.000 for every model.

Table 5 Angle (β) in degree optimization of the weightings (W_1 , W_2 and W_3) and results of turbine efficiency

Case	Angle (degree)											Turbine efficiency		
	W_1	W_2	W_3	β_1	β_2	β_3	β_4	β_5	β_6	β_7	β_8	Q (m ³ /s)	H_{total} (m)	η (%)
1	0.1	0.5	0.4	13.6	20.1	30.0	40.1	31.1	44.9	54.9	55.0	4.97	1.90	80.13
2	0.3	0.2	0.5	10.0	20.0	30.0	40.0	25.0	45.0	48.9	55.0	5.00	1.85	77.22
3	0.5	0.2	0.3	12.9	20.2	30.1	40.0	28.2	45.0	55.0	65.0	4.36	1.93	93.33
4	0.6	0.3	0.1	10.0	20.1	30.2	40.1	27.0	44.9	54.8	64.9	4.39	1.91	93.60
5	0.7	0.1	0.2	11.7	20.2	30.0	40.1	25.6	45.0	55.0	65.0	4.38	1.92	94.14

$Q_c = 5\text{ m}^3/\text{s}$ and the weightings (W_1 , W_2 and W_3).

From Eq. (13), the angle optimization was for a turbine with the head of <2 meters and the flow rate

of <5 m³ /s. The initial step was to obtain the weightings (W_1 , W_2 and W_3) by considering the angle between guide vane and turbine blade, with optimized turbine efficiency for 1 run.

From Table 5, it was obvious that case 5 gave the

Table 6 Angle (β) in degree optimization with 10 runs from the weightings (0.7, 0.1 and 0.2) and their results

Run	Angle (degree)								Results		
	β_1	β_2	β_3	β_4	β_5	β_6	β_7	β_8	Q (m ³ /s)	H_{total} (m)	η (%)
1	11.7	20.2	30.0	40.1	25.6	45.0	55.0	65.0	4.38	1.92	94.14
2	10.0	20.0	30.0	40.0	26.5	42.1	55.0	65.0	4.42	1.88	93.58
3	11.5	20.2	30.1	40.1	25.3	44.5	54.9	65.0	4.38	1.91	94.01
4	13.3	20.1	30.0	40.5	25.0	44.9	55.0	65.0	4.36	1.91	94.09
5	11.7	20.0	30.0	40.1	25.0	44.8	55.0	65.0	4.38	1.91	94.34
6	10.2	20.2	30.2	40.0	26.0	45.0	55.0	65.0	4.38	1.91	94.10
7	10.1	20.0	30.0	40.5	25.0	45.0	55.0	65.0	4.37	1.91	94.43
8	10.0	20.2	30.1	45.8	25.0	44.3	55.0	65.0	4.23	1.89	93.12
9	10.0	20.2	30.1	40.2	25.2	44.8	55.0	65.0	4.38	1.91	94.32
10	10.4	20.0	30.0	40.1	25.0	41.3	55.0	65.0	4.44	1.87	93.69

Table 7 Comparison between the optimization method and the CFD

Model	Q (m ³ /s)	H_{total} (m)	η (%)	Output (kW)
Optimization	4.37	1.91	94.43	77.18
CFD	4.20	2	83.96	69.06
Total difference (%)	-4.04	4.50	-12.47	-11.75

maximum efficiency of 94.14%, with the optimal weightings (W_1 , W_2 and W_3) of 0.7, 0.1, and 0.2, respectively.

In the following step, the weighting from the initial step was optimized for the angle between guide vane and turbine blade with 10 runs (Table 6), as well as the results of flow rate, total head and performance. The seventh run obtained the maximum efficiency of 94.43% and the angles of the guide vane and the turbine blade, β_1 to β_8 , were 10.1°, 20°, 30°, 40.5°, 25°, 45°, 55°, and 65° respectively.

Table 7 confirmed that the optimization method successfully improved the turbine efficiency of the original design of the CFD simulation. The CFD efficiency was increased to 83.96% when the flow rate was 4.2 m³/s and the total head was 2 meters. The total difference between the optimization method and the CFD simulation, for the flow rate, total head, efficacy and output power were -4.04%, 4.5%, -12.47% and -11.75% respectively.

6. CONCLUSIONS

CFD simulation method was successfully applied to solve the flow problem in the axial turbine, giving results for the regression analysis to develop mathematical models of turbine behavior. The guide vane angles and the turbine blade angles were variables in equations, expressing the turbine efficiency, total head and flow rate. The optimal equation of relationships between the angle of guide vane and turbine blade as functions of performance

and flow rate is the multiple linear regression, while that as functions of total head is non-linear double log. The multi-objective function by using GA was also employed in the angle optimization, obtaining the optimal blade angles β_1 to β_8 of 10.1°, 20°, 30°, 40.5°, 25°, 45°, 55°, and 65° respectively, and improving the turbine efficiency to 94.43%. The efficiency was 83.96% for subsequent CFD simulations. Total efficiency difference of the simulation and the optimization was -12.47%. Still, the optimization method can also be utilized to improve the turbine efficiency of the original design.

REFERENCES

- Albuquerque, R. B. F., N. Manzanara-Filho and W. Oliveira (2007). Conceptual optimization of axial-flow hydraulic turbines with non-free vortex design. *Journal of Power and Energy-Part A* 221 713–725.
- Alexander, K. V., E. P. Giddens and A. M. Fuller (2009). Axial-flow turbines for low head microhydro systems. *Renewable Energy* 34, 35–47.
- Alnaga, A. and J. L. Kueny (2008). Optimal Design of Hydraulic Turbine Distributor. *Wseas Transactions on Fluid mechanics* 3(2), 175–185.
- Benajes, J., J. Galindo, P. Fajardo and R. Navarro (2014). Development of a Segregated Compressible Flow Solver for Turbomachinery Simulations. *Journal of Applied Fluid*

- Mechanics* 7(4), 673–682.
- Chakraborty, A. (2015). Latin Hypercube Sampling: Structural Reliability. URL: <http://nptel.ac.in/courses/105103140/module4/3.pdf>
- Chen, N., H. Zhang, W. Huang and Y. Xu (2005). Study on aerodynamic design optimization of turbomachinery blades. *Journal of Thermal Science* 14(4), 298–304.
- Ferro, L. M. C., L. M. C. Gato and A. F. O. Falcão (2011). Design of the rotor blades of a mini hydraulic bulb-turbine. *Renewable Energy* 36, 2395–2403.
- Ge, X., Y. Feng, Y. Zhou, Y. Zheng and C. Yang (2013). Optimization Study of Shaft Tubular Turbine in a Bidirectional Tidal Power Station. *Advances in Mechanical Engineering*.
- Jung, I. S., W. H. Jung, S. H. Baek and S. Kang (2012). Shape Optimization of Impeller Blades for a Bidirectional Axial Flow Pump using Polynomial Surrogate Model. *World Academy of Science, Engineering and Technology* 66, 718–724.
- Kaniecki, M., Z. Krzemianowski and M. Banaszek (2011). Computational fluid dynamics simulations of small capacity Kaplan turbines. *Transaction of the Institute of Fluid-Flow Machinery* 123, 71–84.
- Lazari, A. and A. Cattanei (2014). Design of off-statistics axial-flow fans by means of vortex law optimization. *Journal of Thermal Science* 23(6), 505–515.
- Lipej, A. (2004). Optimization method for the design of axial hydraulic turbines. *Journal of Power and Energy-Part A* 218, 43–50.
- Mokaramian, A., V. Rasouli and G. Cavanaugh (2015). Turbodrill Design and Performance Analysis. *Journal of Applied Fluid Mechanics* 8(3), 377–390.
- Pires, J. C. M., F. G. Martins, S. I. V. Sousa, M. C. M. Alvim-Ferraz and M. C. Pereira (2008). Selection and validation of parameters in multiple linear and principal component regressions. *Environmental Modelling and Software* 23, 50–55.
- Ramos, M., H. Mariana Simão and A. Borga (2013). Experiments and CFD Analyses for a New Reaction Microhydro Propeller with Five Blades. *Journal of Energy Engineering* 139, 109–117.
- Round, F. G. (2004). Some aspects of design: Incompressible flow turbomachine. Elsevier Inc, Oxford, UK.
- Singh, P. and F. Nestmann (2011). Experimental investigation of the influence of blade height and blade number on the performance of low head axial flow turbines. *Renewable Energy* 36, 272–281.
- Skotak, A., J. Mikulasek and J. Obrovsky (2009). Development of The New High Specific Speed Fixed Blade Turbine Runner. *International Journal of Fluid Machinery and Systems* 2(4), 392–399.
- Sun, S. and J. L. Bertrand-Krajewski (2012). On calibration data selection: The case of stormwater quality regression models. *Environmental Modelling and Software* 35, 61–73.
- Sutikno, P. and I. K. Adam (2011). Design, simulation and experimental of the very low head turbine with minimum pressure and free vortex criterions. *International Journal of Mechanical and Mechatronics Engineering* 11(1), 9–16.
- Wu, J., K. Shimmei, K. Tani, J. Sato and K. Niikura (2006). CFD-Based Design Optimization for Hydro Turbines. *Journal of Fluids Engineering* 129, 159–168.
- Yang, W., Y. Wu and S. Liu (2011). An optimization method on runner blades in bulb turbine based on CFD analysis. *Science China Technological Sciences* 54(2), 338–344.